International Journal of Scientific and Technical Advancements
IJSTA
ISSN: 2454-1532

An Optimized and Robust Iris Recognition Algorithm for Biometric Authentication Systems

Kanika Sharma[1,#], Randhir Singh[1]
[1]Department of Electronics and Communication Engineering, Sri Sai College of Engineering and Technology, Badhani, Pathankot, India
[#]Email address: kanikas.horizon@gmail.com

Abstract—Biometric authentication systems are based on the concept of matching some unique features of human body such as fingerprints, facial features, hand geometry, speech etc. One such feature viz. the Iris, a thing circular diaphragm lying between the cornea and retina of human eye, has been considered in this paper. A new optimized and robust iris recognition algorithm has been proposed in this paper for application in various biometric authentication applications. The acquired image first undergoes segmentation using the circular Hough transform for localizing the iris and pupil regions, and the linear Hough transform for localizing occluding eyelids. Next, the segmented iris region will be normalized by Daugman's rubber sheet model to eliminate dimensional inconsistencies between iris regions. Finally, features of the iris will be encoded by convolving the normalized iris region with 1-D Log-Gabor filters and phase quantizing the output in order to produce a bit-wise biometric template. The Hamming distance is proposed to be chosen as a matching metric, which can give a measure of how many bits disagree between two templates. Based on the simulation results, it is observed that the proposed algorithm works accurately for different test images and thus can be used in different biomedical applications.

Keywords— Iris Recognition, Biometric Authentication, Image Processing, Segmentation, Feature Extraction

I. INTRODUCTION

A biometric authentication system provides automatic recognition of an individual based on some sort of unique feature or characteristic possessed by the individual. Biometric systems work by first capturing a sample of the feature, such as recording a digital sound signal for voice recognition, or taking a digital colour image for face recognition. The sample is then transformed using some sort of mathematical function into a biometric template. The biometric template will provide a normalised, efficient and highly discriminating representation of the feature, which can then be objectively compared with other templates in order to determine identity. Biometric systems have been developed based on fingerprints [1,2], facial features [3,4], voice [5,6], hand geometry [7,8], the retina [9,10], and the one presented in this paper, the iris.

The iris is a thin circular diaphragm, which lies between the cornea and the lens of the human eye. The function of the iris is to control the amount of light entering through the pupil, and this is done by the sphincter and the dilator muscles, which adjust the size of the pupil. The average diameter of the iris is 12 mm, and the pupil size can vary from 10% to 80% of the iris diameter. The iris is an externally visible, yet protected organ whose unique epigenetic pattern remains stable throughout adult life. These characteristics make it very attractive for use as a biometric for identifying individuals. Image processing techniques can be employed to extract the unique iris pattern from a digitised image of the eye, and encode it into a biometric template, which can be stored in a database. This biometric template contains an objective mathematical representation of the unique information stored in the iris, and allows comparisons to be made between templates. When a subject wishes to be identified by an iris recognition system, their eye is first photographed, and then a template created for their iris region. This template is then compared with the other templates stored in a database until either a matching template is found and the subject is identified, or no match is found and the subject remains unidentified.

II. LITERATURE REVIEW

In [11] authors have proposed modified Log-Gabor filters for iris recognition. The proposed filter in general is similar to Daugman algorithm proposed in [12] but the Log-Gabor filters are used to extract the iris phase information instead of complex Gabor filters used in Daugman's [12]. The advantage of Log-Gabor filters over complex Gabor filters is the former are strictly bandpass filters and the latter are not. The property of strictly bandpass makes the Log-Gabor filters more suitable to extract the iris phase features regardless of the background brightness. Special attention has not been paid to a modified system in which a more accurate segmentation process is applied to an already existing efficient algorithm thereby increasing the overall reliability and accuracy of iris recognition. In [13] an improvement of the already existing wavelet packet decomposition for iris recognition with a Correct Classification Rate (CCR) is proposed. It involves changing the segmentation technique used for this implementation from the integro-differential operator approach (John Daugman's model [12]) to the Hough transform (Wilde's model). This research extensively compared the two segmentation techniques to show which is better in the implementation of the wavelet packet decomposition. Vatsa et al. [14] proposed algorithms for iris segmentation, quality enhancement, match score fusion, and indexing to improve both the accuracy and the speed of iris recognition. A curve evolution approach is proposed to

Kanika Sharma and Randhir Singh, "An optimized and robust iris recognition algorithm for biometric authentication systems," *International Journal of Scientific and Technical Advancements*, Volume 4, Issue 4, pp. 1-8, 2018.

effectively segment a non-ideal iris image using the modified Mumford-Shah functional. Different enhancement algorithms are concurrently applied on the segmented iris image to produce multiple enhanced versions of the iris image. Similarly in [15], two powerful sets of features are introduced to be used for iris recognition: scattering transform-based features and textural features. PCA is also applied on the extracted features to reduce the dimensionality of the feature vector while preserving most of the information of its initial value. A new iris recognition algorithm is proposed in [16], which adopts Independent Component Analysis (ICA) to extract iris texture feature and a competitive learning mechanism to recognize iris patterns. Experimental results show that the algorithm is efficient and adaptive to the environment, e.g. it works well even for blurred iris images, variable illumination, and interference of eyelids and eyelashes.

III. PROPOSED METHODOLOGY

The proposed iris recognition is shown in Fig. 1. Firstly, an automatic segmentation algorithm will be proposed, which would localize the iris region from an eye image and isolate eyelid, eyelash and reflection areas. Automatic segmentation is proposed to be achieved through the use of the circular Hough transform for localizing the iris and pupil regions, and the linear Hough transform for localizing occluding eyelids. Thresholding will be employed for isolating eyelashes and reflections.

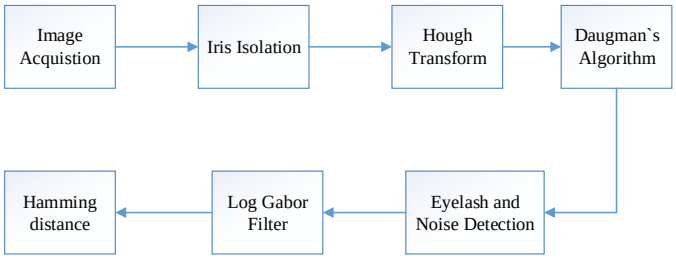

Fig. 1. Proposed Iris Recognition System

Next, the segmented iris region will be normalized to eliminate dimensional inconsistencies between iris regions. This normalization is proposed to be achieved by implementing a version of Daugman's rubber sheet model, where the iris is modelled as a flexible rubber sheet, which is unwrapped into a rectangular block with constant polar dimensions.

Finally, features of the iris will be encoded by convolving the normalized iris region with 1-D Log-Gabor filters and phase quantizing the output in order to produce a bit-wise biometric template. The Hamming distance is proposed to be chosen as a matching metric, which can give a measure of how many bits disagree between two templates. A failure of statistical independence between two templates would result in a match, that is, the two templates were deemed to have been generated from the same iris if the Hamming distance produced was lower than a set Hamming distance.

A. *Segmentation*

The first stage of iris recognition is to isolate the actual iris region in a digital eye image. The iris region, shown in Figure 1.1, can be approximated by two circles, one for the iris/sclera boundary and another, interior to the first, for the iris/pupil boundary. The eyelids and eyelashes normally occlude the upper and lower parts of the iris region. Also, specular reflections can occur within the iris region corrupting the iris pattern. A technique is required to isolate and exclude these artefacts as well as locating the circular iris region.

It was decided to use circular Hough transform for detecting the iris and pupil boundaries. This involves first employing Canny edge detection to generate an edge map. Gradients were biased in the vertical direction for the outer iris/sclera boundary. Vertical and horizontal gradients were weighted equally for the inner iris/pupil boundary. The Hough transform is a standard computer vision algorithm that can be used to determine the parameters of simple geometric objects, such as lines and circles, present in an image. The circular Hough transform can be employed to deduce the radius and centre coordinates of the pupil and iris regions. Firstly, an edge map is generated by calculating the first derivatives of intensity values in an eye image and then thresholding the result. From the edge map, votes are cast in Hough space for the parameters of passing through each edge point. These parameters are the centre coordinates x_c and y_c and the radius r, which are able to define any circle according to the equation

$$x_c^2 + y_c^2 - r^2 = 0$$

A maximum point in the Hough space will correspond to the radius and centre co-ordinates of the circle best defined by the edge point, also make use of the parabolic Hough transform to detect the eyelids, approximating the upper and lower eyelids with parabolic arcs, which are represented as

$$\left(-\left(x-h_j\right)\sin\theta_j+\left(y-k_j\right)\cos\theta_j\right)^2 = a_j\left(\left(x-h_j\right)\cos\theta_j+\left(y-k_j\right)\sin\theta_j\right)$$

where a_j controls the curvature, (h_j, k_j) is the peak of the parabola and θ_j is the angle of rotation relative to the x-axis.

In performing the preceding edge detection step, bias the derivatives in the horizontal direction for detecting the eyelids, and in the vertical direction for detecting the outer circular boundary of the iris, this is illustrated in Fig. 2.

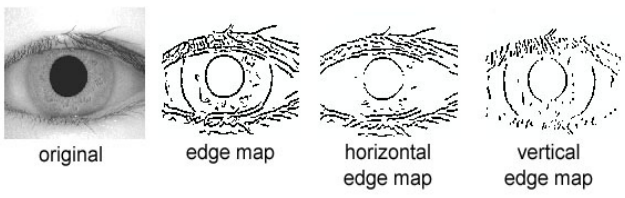

Fig 2- Edge detection illustration **a)** an eye image **b)**

Kanika Sharma and Randhir Singh, "An optimized and robust iris recognition algorithm for biometric authentication systems," *International Journal of Scientific and Technical Advancements*, Volume 4, Issue 4, pp. 1-8, 2018.

ISSN: 2454-1532

corresponding edge map **c)** edge map with only horizontal gradients **d)** edge map with only vertical gradients.

The motivation for this is that the eyelids are usually horizontally aligned, and also the eyelid edge map will corrupt the circular iris boundary edge map if using all gradient data. Taking only the vertical gradients for locating the iris boundary will reduce influence of the eyelids when performing circular Hough transform, and not all of the edge pixels defining the circle are required for successful localisation. Not only does this make circle localisation more accurate, it also makes it more efficient, since there are less edge points to cast votes in the Hough space.

The range of radius values to search for was set manually, depending on the database used. In order to make the circle detection process more efficient and accurate, the Hough transform for the iris/sclera boundary was performed first, then the Hough transform for the iris/pupil boundary was performed within the iris region, instead of the whole eye region, since the pupil is always within the iris region. After this process was complete, six parameters are stored, the radius, and *x* and *y* centre coordinates for both circles.

Eyelids were isolated by first fitting a line to the upper and lower eyelid using the linear Hough transform. A second horizontal line is then drawn, which intersects with the first line at the iris edge that is closest to the pupil. This process is illustrated in Fig. 3 and Fig. 4 and is done for both the top and bottom eyelids. The second horizontal line allows maximum isolation of eyelid regions. Canny edge detection is used to create an edge map, and only horizontal gradient information is taken. The linear Hough transform is implemented using the MATLAB Radon transform, which is a form of the Hough transform. If the maximum in Hough space is lower than a set threshold, then no line is fitted, since this corresponds to non-occluding eyelids. Also, the lines are restricted to lie exterior to the pupil region, and interior to the iris region. A linear Hough transform has the advantage over its parabolic version, in that there are less parameters to deduce, making the process less computationally demanding.

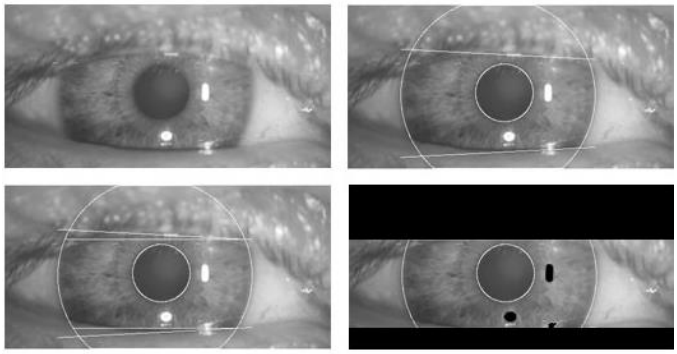

Fig 3 - Stages of segmentation with eye image **Top left**) original eye image **Top right)** two circles overlayed for iris and pupil boundaries, and two lines for top and bottom eyelid **Bottom left)** horizontal lines are drawn for each eyelid from the lowest/highest point of the fitted line **Bottom right)** probable eyelid and specular reflection areas isolated (black areas)

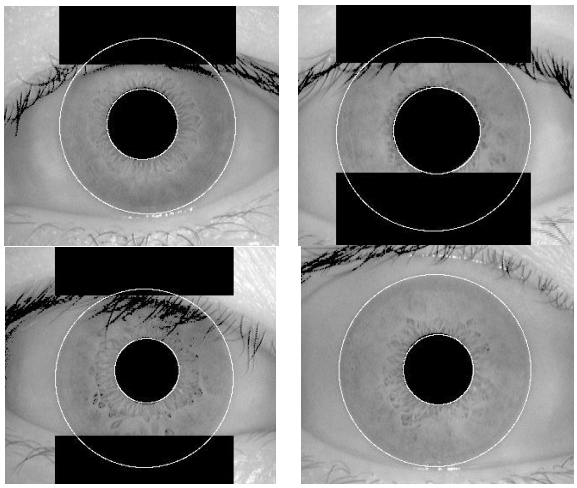

Fig 4 - Automatic segmentation of various images from the database. Black regions denote detected eyelid and eyelash regions.

B. Normalization

Once the iris region is successfully segmented from an eye image, the next stage is to transform the iris region so that it has fixed dimensions in order to allow comparisons. The dimensional inconsistencies between eye images are mainly due to the stretching of the iris caused by pupil dilation from varying levels of illumination. Other sources of inconsistency include, varying imaging distance, rotation of the camera, head tilt, and rotation of the eye within the eye socket. The normalisation process will produce iris regions, which have the same constant dimensions, so that two photographs of the same iris under different conditions will have characteristic features at the same spatial location. For normalisation of iris regions a technique based on Daugman's rubber sheet model was employed.

The homogenous rubber sheet model, shown in Fig. 5, devised by Daugman remaps each point within the iris region to a pair of polar coordinates (r, θ) where r is on the interval [0,1] and θ is angle [0, 2θ].

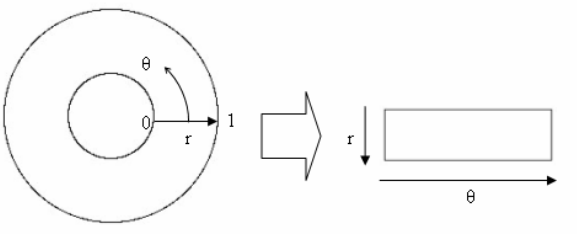

Fig 5 - Daugman's rubber sheet model.

The remapping of the iris region from *(x,y)* Cartesian coordinates to the normalised non-concentric polar representation is modelled as

Kanika Sharma and Randhir Singh, "An optimized and robust iris recognition algorithm for biometric authentication systems," *International Journal of Scientific and Technical Advancements*, Volume 4, Issue 4, pp. 1-8, 2018.

ISSN: 2454-1532

$$I\left(x(r,\theta),y(r,\theta)\right)\rightarrow I(r,\theta)$$

With

$$x(r,\theta)=(1-r)\,x_p(\theta)+r x_l(\theta)$$
$$y(r,\theta)=(1-r)\,y_p(\theta)+r y_l(\theta)$$

where *I(x,y)* is the iris region image, *(x,y)* are the original Cartesian coordinates, *(r,θ)* are the corresponding normalised polar coordinates, and x_p , y_p and x_l , y_l are the coordinates of the pupil and iris boundaries along the θ direction. The rubber sheet model takes into account pupil dilation and size inconsistencies in order to produce a normalised representation with constant dimensions. In this way the iris region is modelled as a flexible rubber sheet anchored at the iris boundary with the pupil centre as the reference point. Even though the homogenous rubber sheet model accounts for pupil dilation, imaging distance and non-concentric pupil displacement, it does not compensate for rotational inconsistencies. In the Daugman system, rotation is accounted for during matching by shifting the iris templates in the θ direction until two iris templates are aligned.

The centre of the pupil was considered as the reference point, and radial vectors pass through the iris region, as shown in Fig. 6. A number of data points are selected along each radial line and this is defined as the radial resolution. The number of radial lines going around the iris region is defined as the angular . Since the pupil can be non-concentric to the iris, a remapping formula is needed to rescale points depending on the angle around the circle. This is given by

$$r' = \sqrt{\alpha}\beta \pm \sqrt{\alpha\beta^2-\alpha-r_I^2}$$

With

$$\alpha = o_x^2 + o_y^2$$
$$\beta = \cos\left(\pi - \arctan\left(\frac{o_y}{o_x}\right) - \theta\right)$$

where displacement of the centre of the pupil relative to the centre of the iris is given by o_x, o_y and r' is the distance between the edge of the pupil and edge of the iris at an angle, θaround the region, and r_I is the radius of the iris. The remapping formula first gives the radius of the iris region 'doughnut' as a function of the angle θ.

A constant number of points are chosen along each radial line, so that a constant number of radial data points are taken, irrespective of how narrow or wide the radius is at a particular angle. The normalised pattern was created by backtracking to find the Cartesian coordinates of data points from the radial and angular position in the normalised pattern. From the 'doughnut' iris region, normalisation produces a 2D array with horizontal dimensions of angular resolution and vertical dimensions of radial resolution. Another 2D array was created for marking reflections, eyelashes, and eyelids detected in the segmentation stage. In order to prevent non-iris region data from corrupting the normalised representation, data points which occur along the pupil border or the iris border are discarded. As in Daugman's rubber sheet model, removing rotational inconsistencies is performed at the matching stage.

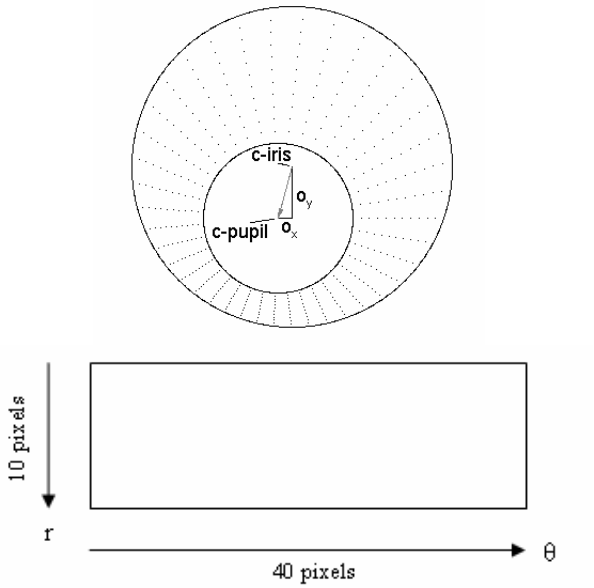

Fig. 6 - Outline of the normalisation process with radial resolution of 10 pixels, and angular resolution of 40 pixels. Pupil displacement relative to the iris centre is exaggerated for illustration purposes.

Normalisation of two eye images of the same iris is shown in Fig. 7. The pupil is smaller in the bottom image, however the normalisation process is able to rescale the iris region so that it has constant dimension. In this example, the rectangular representation is constructed from 10,000 data points in each iris region. Note that rotational inconsistencies have not been accounted for by the normalisation process, and the two normalised patterns are slightly misaligned in the horizontal (angular) direction. Rotational inconsistencies will be accounted for in the matching stage.

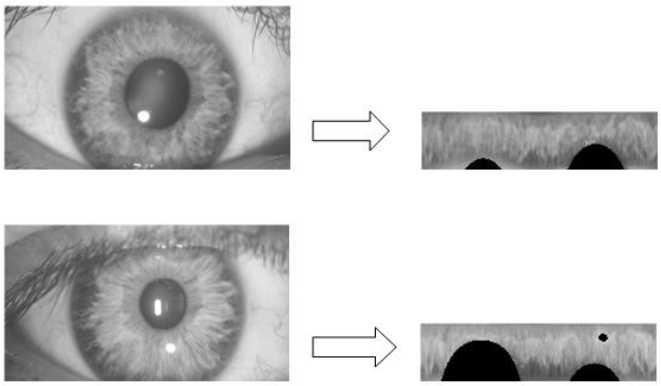

Fig. 7 - Illustration of the normalisation process for two images of the same iris taken under varying conditions.

Kanika Sharma and Randhir Singh, "An optimized and robust iris recognition algorithm for biometric authentication systems," *International Journal of Scientific and Technical Advancements*, Volume 4, Issue 4, pp. 1-8, 2018.

ISSN: 2454-1532

C. Feature Encoding

In order to provide accurate recognition of individuals, the most discriminating information present in an iris pattern must be extracted. Only the significant features of the iris must be encoded so that comparisons between templates can be made. Most iris recognition systems make use of a band pass decomposition of the iris image to create a biometric template. Feature encoding was implemented by convolving the normalised iris pattern with 1D Log-Gabor wavelets.

Gabor filters are able to provide optimum conjoint representation of a signal in space and spatial frequency. A Gabor filter is constructed by modulating a sine/cosine wave with a Gaussian. This is able to provide the optimum conjoint localisation in both space and frequency, since a sine wave is perfectly localised in frequency, but not localised in space. Modulation of the sine with a Gaussian provides localisation in space, though with loss of localisation in frequency. Decomposition of a signal is accomplished using a quadrature pair of Gabor filters, with a real part specified by a cosine modulated by a Gaussian, and an imaginary part specified by a sine modulated by a Gaussian. The real and imaginary filters are also known as the even symmetric and odd symmetric components respectively.

The centre frequency of the filter is specified by the frequency of the sine/cosine wave, and the bandwidth of the filter is specified by the width of the Gaussian. Daugman makes uses of a 2D version of Gabor filters in order to encode iris pattern data. A 2D Gabor filter over the an image domain *(x,y)* is represented as

$$G(x,y) = e^{-\pi\left[(x-x_0)^2/\alpha^2+(y-y_0)^2/\beta^2\right]} e^{-2\pi i\left[u_0(x-x_0)+v_0(y-y_0)\right]}$$

where (x_o, y_o) specify position in the image, (α,β) specify the effective width and length, and (u_o,v_o) specify modulation. The odd symmetric and even symmetric 2D Gabor filters are shown in Fig. 8.

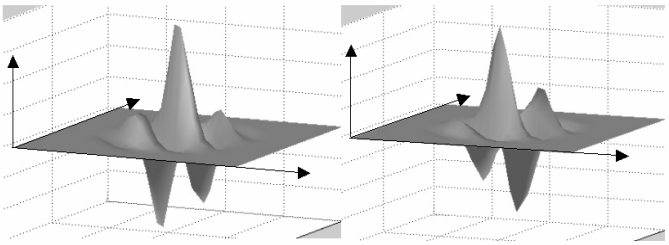

Fig. 8 - A quadrature pair of 2D Gabor filters **left)** real component or even symmetric filter characterised by a cosine modulated by a Gaussian **right)** imaginary component or odd symmetric filter characterised by a sine modulated by a Gaussian.

Daugman demodulates the output of the Gabor filters in order to compress the data. This is done by quantising the phase information into four levels, for each possible quadrant in the complex plane. It has been show that phase information, rather than amplitude information provides the most significant information within an image. Taking only the phase will allow encoding of discriminating information in the iris, while discarding redundant information such as illumination, which is represented by the amplitude component. These four levels are represented using two bits of data, so each pixel in the normalised iris pattern corresponds to two bits of data in the iris template. A total of 2,048 bits are calculated for the template, and an equal number of masking bits are generated in order to mask out corrupted regions within the iris. This creates a compact 256-byte template, which allows for efficient storage and comparison of irises. The Daugman system makes use of polar coordinates for normalisation, therefore in polar form the filters are given as

$$H(r,\theta) = e^{i\omega(\theta_0-\theta_0)} e^{-(r-r_0)^2/\alpha^2} e^{-i(\theta-\theta_0)^2/\beta^2}$$

where (r_0, θ_0) specify the centre frequency of the filter. The demodulation and phase Quantisation process can be represented as

$$h_{\{\mathrm{Re,Im}\}} = \int_{\rho}\int_{\phi} I(\rho,\phi) e^{i\omega(\theta_0-\phi)} e^{-(r_0-\rho)^2/\alpha^2} e^{-(\theta_0-\phi)^2/\beta^2} \rho d\rho d\phi$$

where $h_{\{Re,\ Im\}}$ can be regarded as a complex valued bit whose real and imaginary components are dependent on the sign of the 2D integral, and, $I(\rho,\phi)$ is the raw iris image in a dimensionless polar coordinate system.

The 2D normalised pattern is broken up into a number of 1D signals, and then these 1D signals are convolved with 1D Gabor wavelets. The rows of the 2D normalised pattern are taken as the 1D signal, each row corresponds to a circular ring on the iris region. The angular direction is taken rather than the radial one, which corresponds to columns of the normalised pattern, since maximum independence occurs in the angular direction.

The intensity values at known noise areas in the normalised pattern are set to the average intensity of surrounding pixels to prevent influence of noise in the output of the filtering. The output of filtering is then phase quantised to four levels using the Daugman method, with each filter producing two bits of data for each phasor. The output of phase quantisation is chosen to be a grey code, so that when going from one quadrant to another, only 1 bit changes. This will minimise the number of bits disagreeing, if say two intra-class patterns are slightly misaligned and thus will provide more accurate recognition. The feature encoding process is illustrated in Fig. 9

Kanika Sharma and Randhir Singh, "An optimized and robust iris recognition algorithm for biometric authentication systems," *International Journal of Scientific and Technical Advancements*, Volume 4, Issue 4, pp. 1-8, 2018.

ISSN: 2454-1532

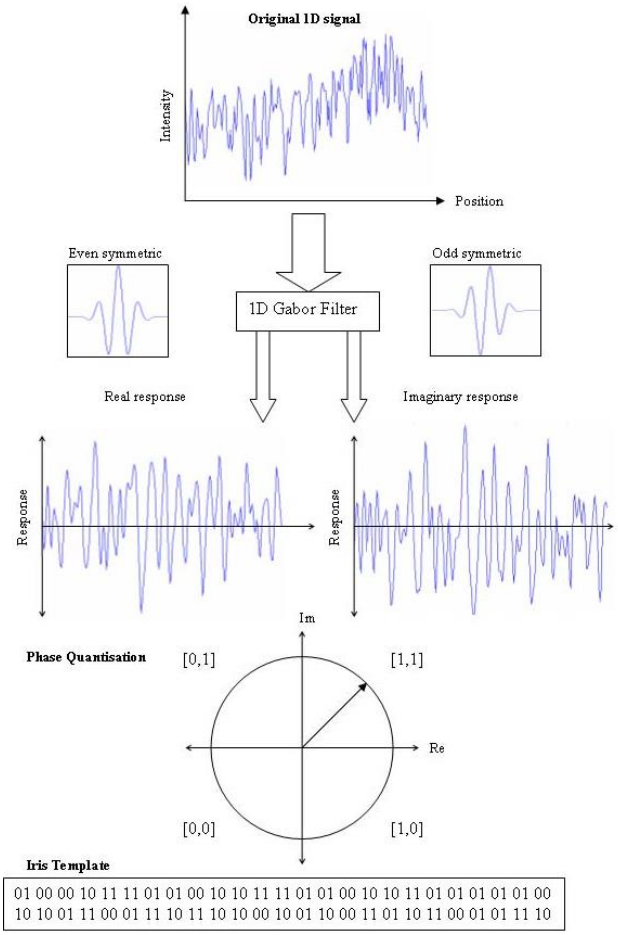

Fig. 9 - An illustration of the feature encoding process.

D. Matching

The template that is generated in the feature encoding process will also need a corresponding matching metric, which gives a measure of similarity between two iris templates. This metric should give one range of values when comparing templates generated from the same eye, known as intra-class comparisons, and another range of values when comparing templates created from different irises, known as inter-class comparisons. These two cases should give distinct and separate values, so that a decision can be made with high confidence as to whether two templates are from the same iris, or from two different irises.

For matching, the Hamming distance was chosen as a metric for recognition, since bit-wise comparisons were necessary. The Hamming distance algorithm employed also incorporates noise masking, so that only significant bits are used in calculating the Hamming distance between two iris templates. Now when taking the Hamming distance, only those bits in the iris pattern that correspond to '0' bits in noise masks of both iris patterns will be used in the calculation. The Hamming distance will be calculated using only the bits generated from the true iris region, and this modified Hamming distance formula is given as

$$HD = \frac{1}{N - \sum_{k=1}^{N} Xn_k\,(OR)\,Yn_k} \sum_{j=1}^{N} X_j\,(XOR)\,Y_j\,(AND)\,Xn'_j\,(AND)\,Yn'_j$$

where X_j and Y_j are the two bit-wise templates to compare, Xn_j and Yn_j are the corresponding noise masks for X_j and Y_j, and N is the number of bits represented by each template.

Although, in theory, two iris templates generated from the same iris will have a Hamming distance of 0.0, in practice this will not occur. Normalisation is not perfect, and also there will be some noise that goes undetected, so some variation will be present when comparing two intra-class iris templates. In order to account for rotational inconsistencies, when the Hamming distance of two templates is calculated, one template is shifted left and right bit-wise and a number of Hamming distance values are calculated from successive shifts. This bit-wise shifting in the horizontal direction corresponds to rotation of the original iris region by an angle given by the angular resolution used. If an angular resolution of 180 is used, each shift will correspond to a rotation of 2 degrees in the iris region. This method is suggested by Daugman, and corrects for misalignments in the normalised iris pattern caused by rotational differences during imaging. From the calculated Hamming distance values, only the lowest is taken, since this corresponds to the best match between two templates.

The number of bits moved during each shift is given by two times the number of filters used, since each filter will generate two bits of information from one pixel of the normalised region. The actual number of shifts required to normalise rotational inconsistencies will be determined by the maximum angle difference between two images of the same eye, and one shift is defined as one shift to the left, followed by one shift to the right. The shifting process for one shift is illustrated in Fig. 10.

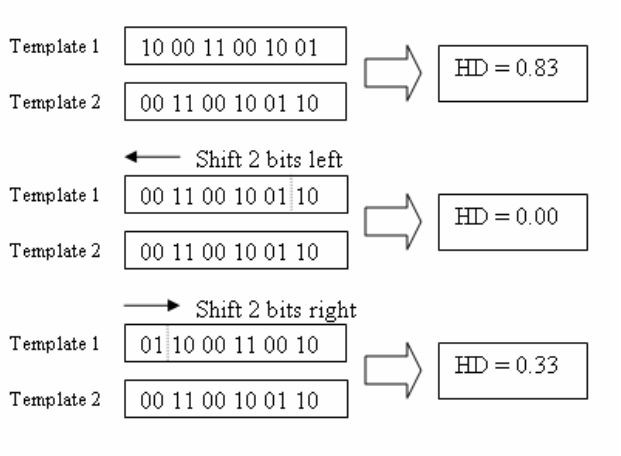

Fig. 10 - An illustration of the shifting process. One shift is defined as one shift left, and one shift right of a reference template. In this example one filter is used to encode the templates, so only two bits are moved during a shift. The lowest Hamming distance, in this case zero, is then used since this corresponds to the best match between the two templates.

Kanika Sharma and Randhir Singh, "An optimized and robust iris recognition algorithm for biometric authentication systems," *International Journal of Scientific and Technical Advancements*, Volume 4, Issue 4, pp. 1-8, 2018.

IV. SIMULATION RESUTLS

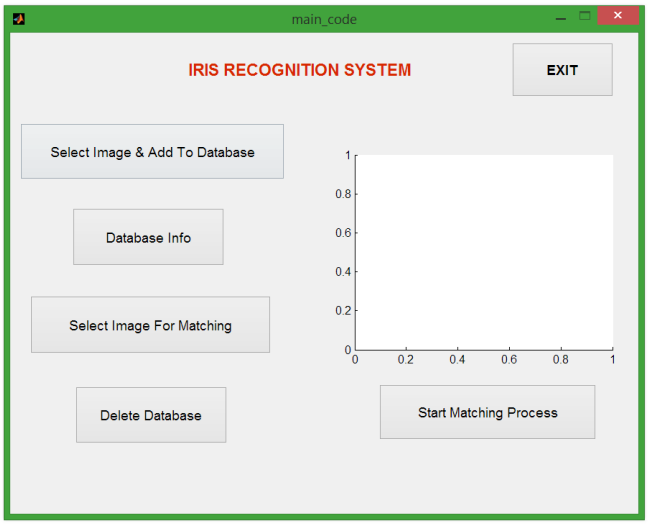

Fig. 11 – GUI of the proposed Iris Recognition System.

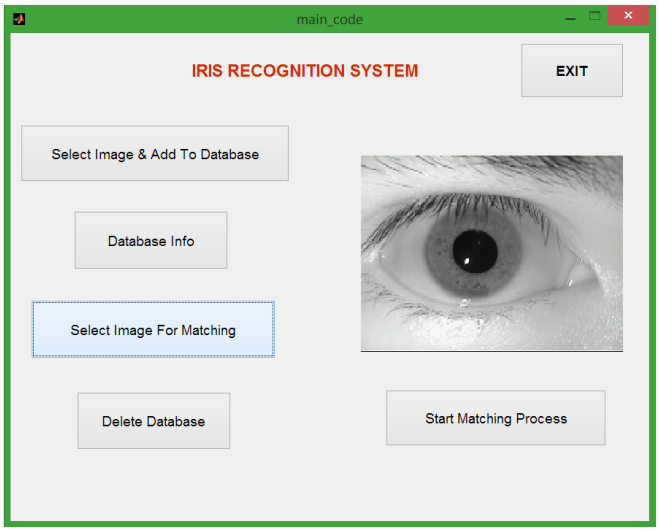

Fig. 12 – Illustration of selection of an eye image for the matching process by the proposed Iris Recognition System.

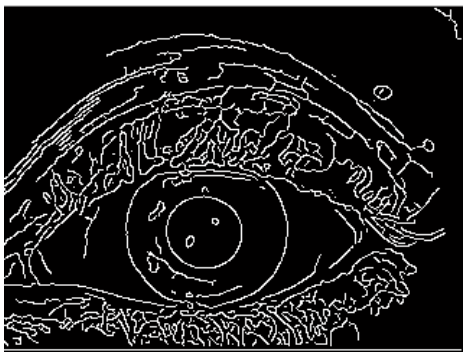

Fig. 13 – Illustration of segmentation of eye image by the proposed Iris Recognition System.

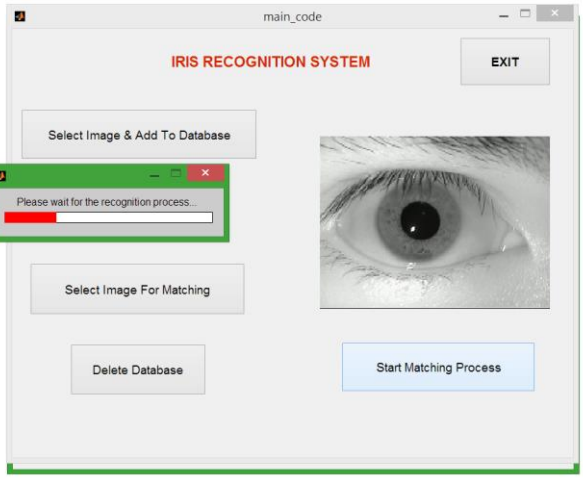

Fig. 14 – Illustration of matching process by the proposed Iris Recognition System.

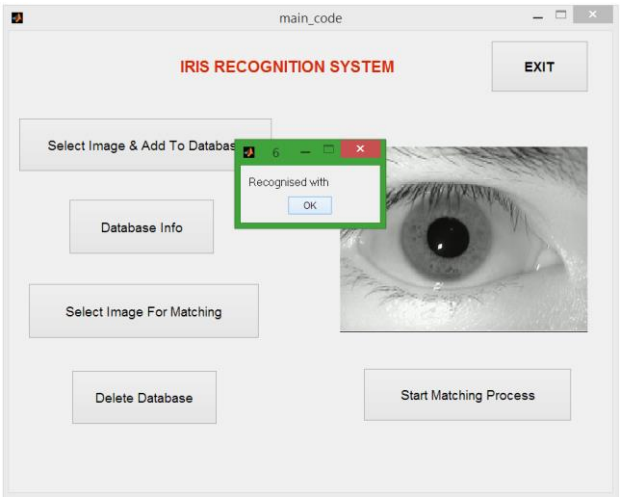

Fig. 15 – Illustration of matching confirmation by the proposed Iris Recognition System.

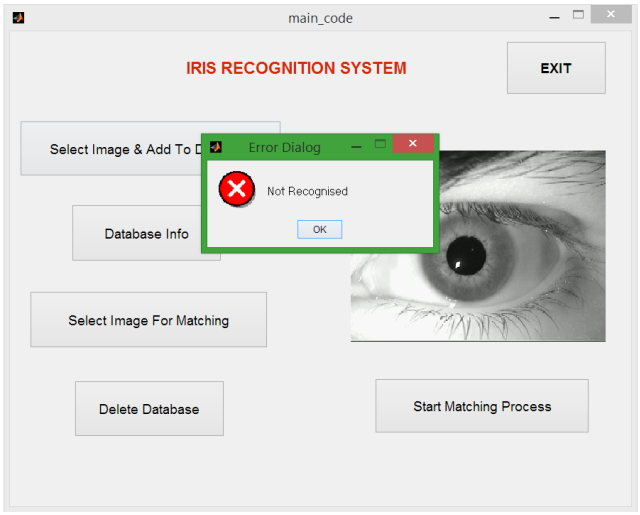

Fig. 16 – Illustration of matching rejection by the proposed Iris Recognition System.

Kanika Sharma and Randhir Singh, "An optimized and robust iris recognition algorithm for biometric authentication systems," *International Journal of Scientific and Technical Advancements*, Volume 4, Issue 4, pp. 1-8, 2018.

V. CONCLUSION

A new optimized and robust iris recognition algorithm has been proposed in this paper for application in various biometric authentication applications. The acquired image first undergoes segmentation using the circular Hough transform for localizing the iris and pupil regions, and the linear Hough transform for localizing occluding eyelids. Next, the segmented iris region will be normalized by Daugman's rubber sheet model to eliminate dimensional inconsistencies between iris regions. Finally, features of the iris will be encoded by convolving the normalized iris region with 1-D Log-Gabor filters and phase quantizing the output in order to produce a bit-wise biometric template. The Hamming distance is proposed to be chosen as a matching metric, which can give a measure of how many bits disagree between two templates. Based on the simulation results, it is observed that the proposed algorithm works accurately for different test images and thus can be used in different biomedical applications.

REFERENCES

[1] James Wayman, Anil Jain, Davide Maltoni, and Dario Maio. "An introduction to biometric authentication systems." In *Biometric Systems*, pp. 1-20. Springer, London, 2005.

[2] Obi Ogbanufe, and Dan J. Kim. "Comparing fingerprint-based biometrics authentication versus traditional authentication methods for e-payment." *Decision Support Systems*, vol. 106, 2018, pp. 1-14.

[3] Marios Savvides, BVK Vijaya Kumar, and Pradeep K. Khosla. "Cancelable biometric filters for face recognition." In *Proc. of the 17th IEEE International Conference on Pattern Recognition*, 2004, pp. 922-925

[4] Wang Feng, Jiyan Zhou, Chen Dan, Zhou Peiyan, and Zhang Li. "Research on mobile commerce payment management based on the face biometric authentication." *International Journal of Mobile Communications*, vol. 15, no. 3, 2017, pp. 278-305.

[5] Girija Chetty and Michael Wagner. "Multi-level liveness verification for face-voice biometric authentication." In proc. of *Biometrics Symposium: Special Session on Research at the IEEE Biometric Consortium Conference*, 2006, pp. 1-6.

[6] Felipe Gomes Barbosa, and Washington Luís Santos Silva. "Support vector machines, Mel-Frequency Cepstral Coefficients and the Discrete Cosine Transform applied on voice based biometric authentication." In proc. of *IEEE SAI Intelligent Systems Conference (IntelliSys), 2015*, pp. 1032-1039.

[7] Puneet Gupta, Saurabh Srivastava, and Phalguni Gupta. "An accurate infrared hand geometry and vein pattern based authentication system." *Knowledge-Based Systems*, vol. 103, 2016, pp. 143-155.

[8] Aditya Nigam and Phalguni Gupta. "Designing an accurate hand biometric based authentication system fusing finger knuckleprint and palmprint." *Neurocomputing*, vol. 151, 2015, pp. 1120-1132.

[9] M. Islamuddin Ahmed, M. Ashraful Amin, Bruce Poon, and Hong Yan. "Retina based biometric authentication using phase congruency." *International Journal of Machine Learning and Cybernetics*, vol. 5, no. 6, 2014, pp. 933-945.

[10] Jarina B. Mazumdar and S. R. Nirmala. "Retina Based Biometric Authentication System: A Review" *International Journal of Advanced Research in Computer Science*, vol. 9, no. 1, 2018, pp. 711-718.

[11] P. Yao, J. Le, X.Ye, Z. Zhuang, B. Li, "Iris Recognition Algorithm using Modified Log-Gabor Filters," *Proc. of IEEE International Conference on Pattern Recognition*, Hong Kong China, 2006, pp. 1-4.

[12] J. Daugman, "How Iris Recognition Works," *IEEE Transactions on Circuits and Systems for Video Technology*, vol. 14, no. 1, 2004, pp. 21-30.

[13] K. Okokpujie, E. Noma-Osaghae, S. Hohn, A. Ajulibe, "An Improved Iris Segmentation Technique using Circular Hough Transform," in *IT Convergence and Security*, Springer, 2017.

[14] M. Vatsa, R. SIgnh, Afzel Noore, "Improving Iris Recognition Performance using Segmentation, Quality Enhancement, Match Score Fusion, and Indexing," *IEEE Transactions on Systems, Man, and Cybernetics, Part B (Cybernetics)*, vol. 38, no. 4, 2008, pp. 1021-1035.

[15] S. Minaee, A. Abdolrashidi, Y. Wang, "Iris recognition using scattering transform and textural features," in proc. of IEEE International Conference on Signal Processing and Signal Processing Education, Salt Lake City, US, 2015.

[16] Y. Huang, S. Luo, E. Chen, "An efficient iris recognition system," in proc. of IEEE International conference on Machine Learning and Cybernetics, Beijing, China, 2002.

Kanika Sharma and Randhir Singh, "An optimized and robust iris recognition algorithm for biometric authentication systems," *International Journal of Scientific and Technical Advancements*, Volume 4, Issue 4, pp. 1-8, 2018.